ELSEVIER

Chemical Engineering Journal 121 (2006) 109–114

Chemical Engineering Journal

www.elsevier.com/locate/cej

Preparation of nano aluminium trihydroxide by high gravity reactive precipitation

Dong-Guang Wang, Fen Guo *, Jian-Feng Chen, Hui Liu, Ze-Ting Zhang

Key Lab for Nanomaterials, Ministry of Education, Research Center of the Ministry of Education for High Gravity Engineering and Technology, Beijing University of Chemical Technology, Beijing 100029, China

Received 29 September 2005; received in revised form 21 May 2006; accepted 22 May 2006

Abstract

Ultra thin hexagonal crystallites of nano aluminium trihydroxide (ATH) with 100–200 nm in particle size and 20–30 nm in thickness have been synthesized by carbonation of sodium aluminate (SA) solution in a rotating packed bed (RPB) reactor, followed by thermal hydrolysis. Due to the intensified absorption of CO_2 under high gravity situations, SA solution was acidified rapidly at a fine scale, and thereby nano-scale gelatinous particles of ATH were precipitated from the supersaturated SA solution. This paper mainly discussed the factors of controlling carbonation process such as carbonation temperature, high gravity level, SA concentration, G/L ratio and terminal pH on the properties of precipitated ATH, which were characterized by TEM, XRD and BET. With carbonation temperature lowered to 30 °C, ATH size sharply reduced to below 200 nm. Higher gravity level and higher G/L favor the absorption of CO_2, resulting in higher supersaturation degree of precursor with the lower pH for nucleation stage. But only when pH values were kept steady in the nucleation stage, the formed particles had a minimum size. In order to achieve ATH crystal phase, the final pH should be above 12.0. When SA concentration rose to 2.0 mol/L, the productivity of ATH achieved 75%.

Keywords: Carbonation; Rotating packed bed; Aluminium trihydroxide; Nanoparticle

1. Introduction

Non-metallurgical aluminium trihydroxide (ATH) is a kind of low-cost, non-toxic, environment friendly, recyclable and crystalline powders. It is the most widely used flame retardant and smoke suppressant in the plastics and rubber industries [1]. It outperforms other solutions in halogen-free wire and cable applications as well as in selected segments of the construction industry [2,3]. ATH/oxides powders are also used in other industry fields such as paper, board, toothpaste, glass, refractories, catalyst, ceramics, medicine, cement, paints, etc. [4]. In recent years, many applications of ATH require finer-sized ATH, because, e.g., high loadings of micron-scale ATH powders often lead to processing difficulties and marked deterioration of mechanical, physical, and electrical properties of the polymers [5,6]. As an alternative, nano ATH powders have been successfully applied to EVA polymer without negatively affecting the properties of the matrix and with a loading of 50 wt.% of nano ATH powders for a better flame retardancy [7]. Therefore, particle size has been the most important index of ATH that determines its quality and value in the market.

Researchers have developed different ways to obtain finer-sized ATH particles. Csige et al. [8] made micron-sized (<1.5–2 μm) ATH by grinding the Bayer precipitates followed by size classification, but the grinding was highly energy-consuming. Direct precipitation from Bayer liquor using seed crystals for submicron-sized ATH (∼250 nm) were also attempted [9]. According to the authors, a lower precipitation temperature and a higher specific surface area of the seed favored the formation of finer particles, and the most important step that influenced the particle size was the addition of a modifier, namely, aluminium sulfate. The particle size was even reduced to ∼1 μm with the addition of a small quantity of aluminium sulfate. Blanks [10] reported on the use of laser-induced localized density fluctuations for stimulating the dehydroxylation of $Al(OH_4^-)$ ions into $Al(OH)_3$ in the absence of seed, and nano-sized ATH (less than 100 nm) had been obtained. The acidification of an aluminate solution with such as $HClO_4$, HNO_3, or CO_2, etc., is another route of synthesizing ATH [11], but reports on this respect are scarce.

* Corresponding author. Tel.: +86 10 64451035; fax: +86 10 64434784.
E-mail address: guof@mail.buct.edu.cn (F. Guo).

1385-8947/$ – see front matter © 2006 Elsevier B.V. All rights reserved.
doi:10.1016/j.cej.2006.05.016

Nomenclature

d_{50}	median size (nm)
g	gravitational acceleration speed (9.8 m/s^2)
G	gas flow rate (m^3/h)
L	liquid flow rate (m^3/h)
N	gravitational acceleration speed in RPB (m/s^2)
T	reaction temperature (°C)

Rotating packed bed (RPB), as a high gravity apparatus for a better multiphase contact, can generate an acceleration of 1–3 orders of magnitude larger than the gravitational acceleration on the earth [12,13]. Since this apparatus can intensify gas–liquid mass transfer and micromixing of fluid, it has been successfully applied to the synthesis of well-defined nano inorganic powders by reactive precipitation method such as calcium carbonate, silica, pseudoboehmite, etc. [14,15]. RPB has obvious advantages over the conventional reactors in production of nano inorganic powders, such as less reaction time, smaller particle size, narrower size distribution as well as easier industrialization, etc.

This paper proposes a process to synthesize nano ATH powders via high gravity reactive precipitation while using CO_2 as acidifier. In the process, sodium aluminate (SA) solution was carbonated by introducing CO_2 into a RPB reactor so that pH gradually decreased to precipitate ATH colloid, which was subsequently treated by thermal hydrolysis to form ultra thin hexagonal crystallites of ATH. It was found that the process is faster and simpler to implement for producing ATH particles of sizes ~150 nm (d_{50}).

2. Experimental

2.1. Materials and equipments

The raw material of ATH used was an industrial product from Shandong Aluminum Corporation, China. Industrial grade sodium hydroxide and food grade CO_2 were used in the experiments. N_2 was used to lower the content of CO_2 as necessary. Analytical grade $Al_2(SO_4)_3{\cdot}18H_2O$ was used as a morphology-control additive. Deionized water was used throughout the study. The carbonation apparatus was illustrated in Fig. 1.

2.2. Experimental procedure

A certain amount of ATH raw material was poured into boiling sodium hydroxide solution. The slurry was kept heating until ATH fully dissolved to obtain raw SA solution, which was subsequently diluted and filtered twice to obtain clear SA solution with a desired concentration. A small amount of morphology-control additive (aluminium sulfate) was added into SA solution. Then the prepared SA solution was poured into the agitating tank, and was forced to circulate between RPB and the agitating tank by a centrifugal pump. CO_2 was introduced into RPB to carbonate SA solution until pH values of the resultant ATH suspension reached a certain value (pH >12.0). Cooling water

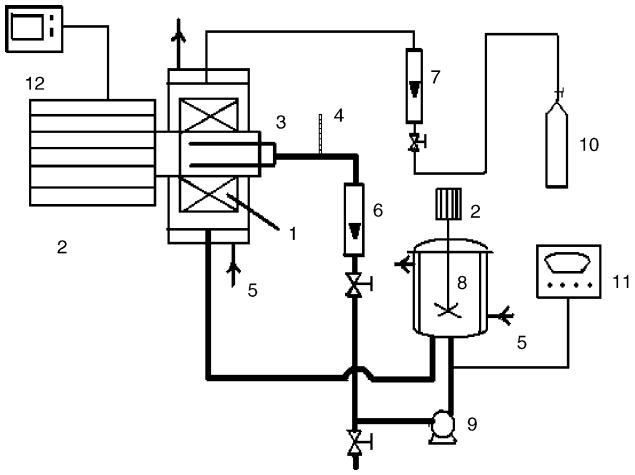

Fig. 1. Experimental set-up of carbonation in RPB: (1) rotating packed bed (RPB); (2) motor; (3) liquid distributor; (4) thermometer; (5) cooling water pipeline; (6) liquid flow meter; (7) gas flow meter; (8) agitating tank; (9) centrifugal pump; (10) CO_2 cylinder; (11) pH meter; (12) frequency modulator.

systems were provided for the RPB and the agitating tank so as to keep the reactive liquor at a constant temperature. After the carbonation, ATH suspension was treated by thermal hydrolysis at 70 °C while vigorously stirring for 3 h. Then the suspension was filtered, rinsed, dried at 110 °C for 8 h and afterwards dispersed to produce nano ATH powders.

Morphological characterisation and particle size measurements were realized by a H-800 Transmission Electron Microscope (HITACHI, Japan). Particle crystal structure analysis was conducted with a HZG4 Multicrystal Diffractometer (Carl Zeiss Jane Company, Germany). BET surface area was determined by ASAP2010 Analyzer (Micromeritics, America).

3. Results and discussion

Nano ATH gel was prepared by controlled carbonation of SA solution in RPB reactor. The process can be expressed as:

I. SA solution is acidified by CO_2 because the concentration of OH^- is very high.

$$2OH^- + CO_2 \rightarrow {CO_3}^{2-} + H_2O \quad (1)$$

II. $Al(OH)_4{}^-$ [16] decomposes and forms $Al(OH)_3$ due to the concentration of OH^- being lowered.

$$Al(OH)_4{}^- \rightarrow Al(OH)_3\downarrow + OH^- \quad (2)$$

The reaction rate of step (1) is controlled by the gas–liquid mass transfer step, and the rate of step (2) is limited by the concentrations of OH^- and $Al(OH)_4{}^-$. During the carbonation, the variation of pH value is an indicator of relative rates of steps (1) and (2). If step (1) is faster than step (2), pH will be lowered; contrarily, pH will be increased. Temperature, high gravity level, SA concentration, G/L ratio and terminal pH value were controlled to achieve the desired products. The effects of various parameters on the carbonation process are discussed below.

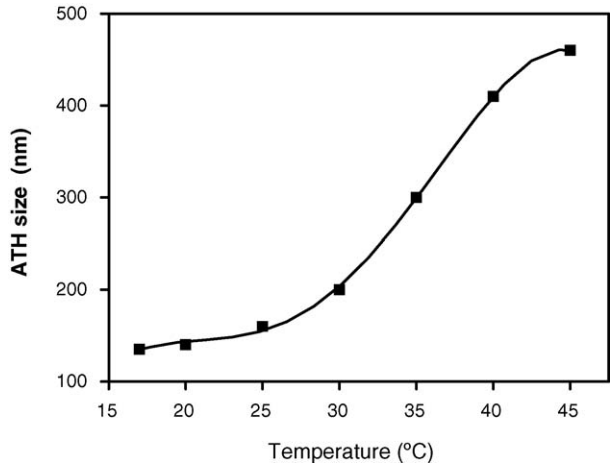

Fig. 2. Effects of temperatures on the particle size of ATH.

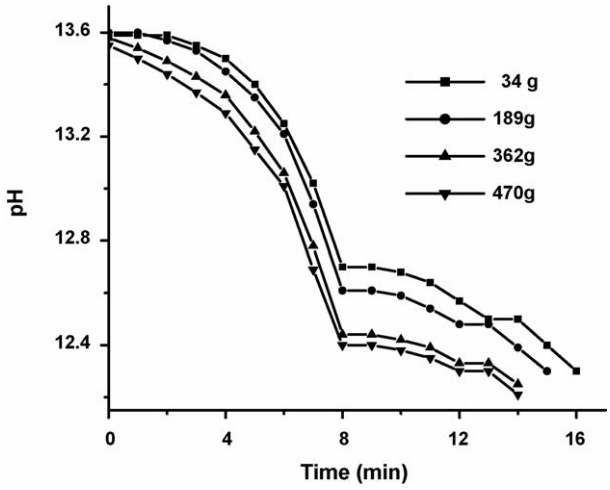

Fig. 4. Effects of high gravity levels on pH variation. Experimental conditions: pure CO_2; [Al(OH$_4^-$)] = 2.0 mol/L; G/L = 1.0; T = 25 °C.

3.1. Carbonation temperature

The effect of temperature on the precipitated ATH were studied in the range of 17–45 °C under the other conditions as: high gravity level 362 g, SA concentration 2.0 mol/L, G/L ratio 1.0, and pure CO_2. Processes were terminated at a pH value of around 12.0. Fig. 2 shows the variation of ATH particle size with carbonation temperatures. It was noted that ATH particle size was significantly reduced when the carbonation temperature was lowered, especially in the range of 30–40 °C. The morphologies of the formed ATH particles were found to be more uniform with process temperatures below 30 °C, see Fig. 3. It was observed that with the decrease of temperature, the viscosity of the resulting ATH suspension after carbonation increased obviously and therefore the period for suspension was prolonged from several minutes to a few days, indicating that low temperature favored the formation of ATH colloid. Therefore, in order to obtain nano ATH, the subsequent carbonation experiments were carried out at temperatures below 30 °C.

3.2. Effect of high gravity level

The effect of high gravity level on the carbonation process was studied in the range of 34–470 g. When the carbonation process was conducted with the use of pure CO_2, it was observed that pH value was lowered faster and carbonation time was shortened at higher gravity levels, see Fig. 4. Obviously, high gravity level is beneficial to the absorption of CO_2 due to an enhanced mass transfer. But this effect is not pronounced when high gravity level is in excess of 362 g. When the carbonation process was conducted with the use of mixed CO_2 of very low concentration (28.6%), pH value was lowered slowly at lower high gravity levels, and it appeared re-increased when high gravity level was lowered to 189 g, see Fig. 5. The increase of pH value appeared at the nucleation moment since the reaction rate of step (2) was accelerated suddenly, and exceeded that of step (1) at this moment. It has been noticed that when pH re-increased, the particle sizes of final products were always large. Therefore, at lower CO_2 concentrations, higher gravity level has definitive effect on the absorption of CO_2.

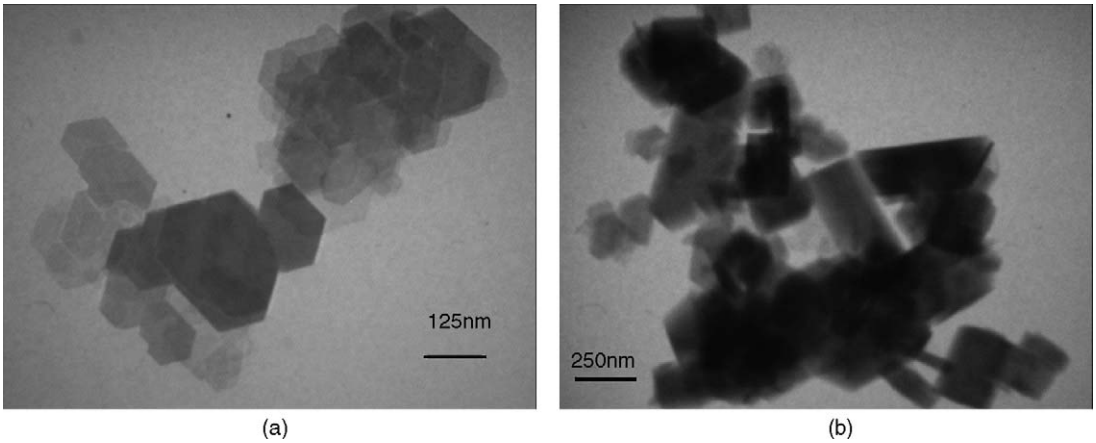

Fig. 3. TEM micrographs of ATH particles prepared by carbonation in RPB at 30 °C (a) and 40 °C (b).

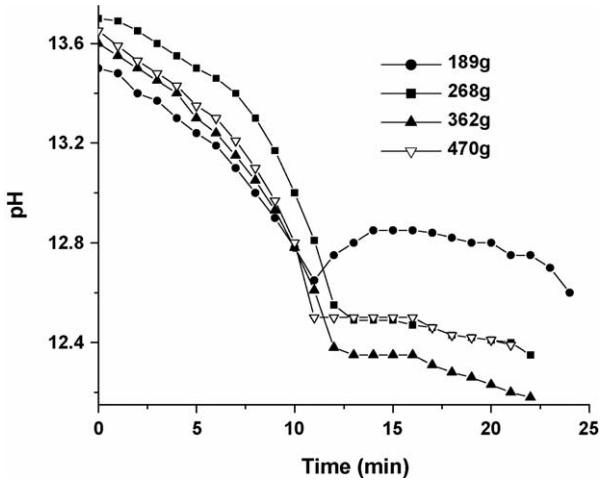

Fig. 5. Effects of high gravity levels on pH variation. Experimental conditions: CO_2 concentration, 28.6%; [Al(OH$_4^-$)] = 2.0 mol/L; G/L = 1.0; T = 25 °C.

3.3. Effect of SA concentration

The effect of SA concentration on the carbonation process was studied in the range of 1.0–3.0 mol/L. Fig. 6 shows the variation of pH value with carbonation time at different SA concentrations. As shown in Fig. 6, at higher SA concentrations, the decrease of pH value was slowered obviously and carbonation time was prolonged markedly. This indicates the decomposition rate of Al(OH$_4^-$) increased at higher SA concentrations. It was noticed that the variation of pH at the nucleation stage showed a gradual decrease from 1.0 to 1.5 mol/L, level off at 2.0 and 2.5 mol/L, and increase at 3.0 mol/L. This implies that the nucleation rate of step (2) varied from slower to faster than the carbonation rate of step (1) with increased SA concentration. Fig. 7 shows the variation of ATH particle sizes and productivity with SA concentrations. In Fig. 7, it is seen that the smallest ATH particle size was in the range of 2.0 and 2.5 mol/L, while ATH productivity increased with higher SA concentrations. The comparison of Fig. 6 with Fig. 7 shows that the precipitated ATH particle size decreased to minimum when pH became steady

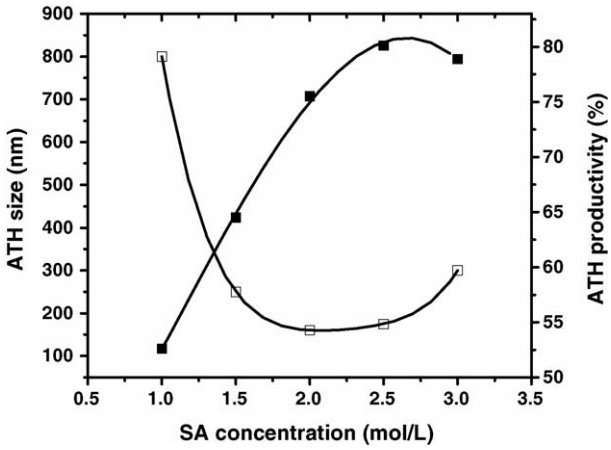

Fig. 7. Effects of SA concentration on ATH productivity and particle size.

at the nucleation moment, i.e., moderate SA concentrations are suitable to produce finer particles at a constant G/L ratio. In addition, it is worth mentioning that when SA concentration was 3.0 mol/L, the created ATH suspension had so high a viscosity as to be discharged very difficultly. Therefore, the optimum SA concentration for the preparation of nano ATH was chosen between 2.0 and 2.5 mol/L.

3.4. Effect of G/L ratio

The effects of G/L ratio on the carbonation process were studied in the range of 0.5–1.25. Fig. 8 shows the variation of pH value with carbonation time at different G/L ratios. SA carbonation time became shorter and pH decreased faster with higher G/L ratios. This shows that higher G/L ratio accelerates the carbonation rate of step (1). Fig. 9 shows the variation of ATH particle size with G/L ratios. It is also observed that the finest product was obtained when pH kept constantly at the nucleation stage. It was believed that under higher G/L ratios the pH difference between RPB and the agitating tank was augmented, in which case ATH nucleation and aggregation occurred simultane-

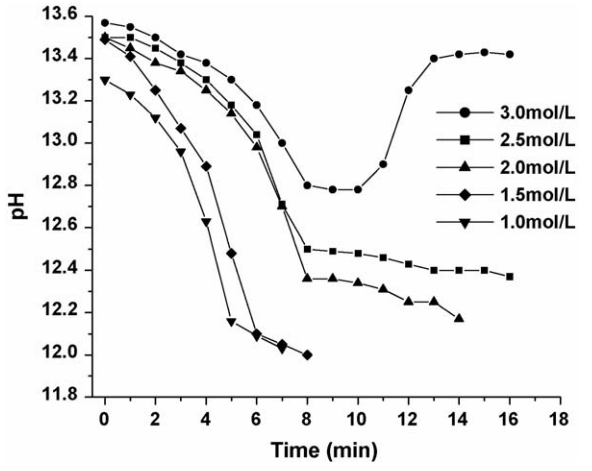

Fig. 6. Effects of SA concentrations on pH variation. Experimental conditions: N = 362 g; G/L = 1.0; T = 25 °C.

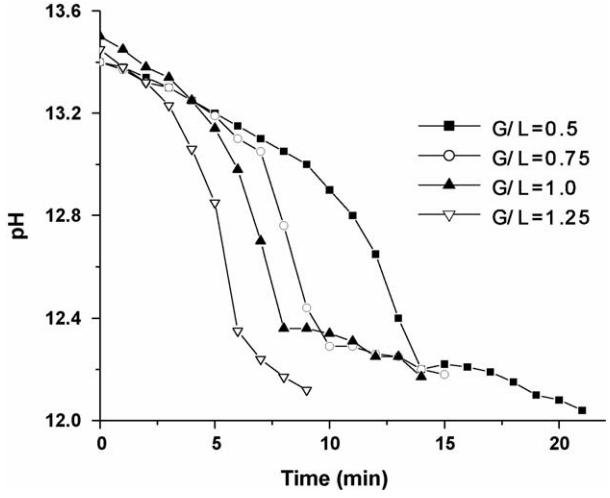

Fig. 8. Effects of G/L ratios on pH variation. Experimental conditions: N = 362 g; [Al(OH$_4^-$)] = 2.0 mol/L; T = 25 °C.

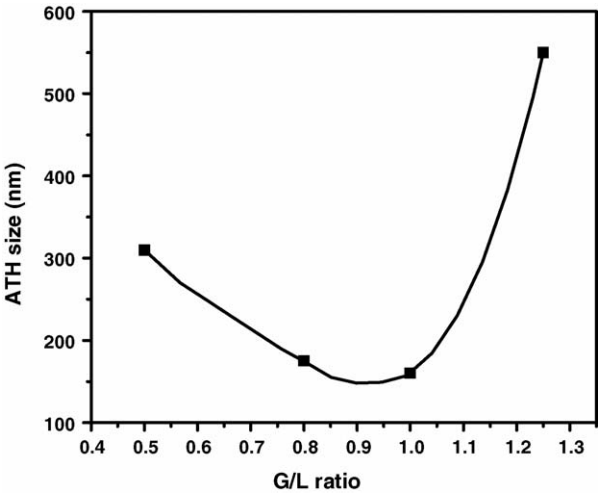

Fig. 9. Effects of G/L ratios on ATH particle size.

ously in RPB. Therefore, moderate G/L ratio should be selected for a finer particle size at constant SA concentration.

3.5. Effect of terminal pH values

XRD patterns of the prepared AH gels indicates that three crystal phases of AH gel were generated at different final pH values, including ATH at final pH 12.0, amorphous precipitate at final pH 12.0–11.0, pseudoboehmite at final pH 11.0–10.0, see Fig. 10. Hence, in order to obtain ATH product, the terminal pH must be controlled to be higher than 12.0.

3.6. Effect of thermal treatment

It has been observed that thermal hydrolysis was in favor of ATH colloids being dehydrated and gelated. The optimum treatment time of 3 h and optimum temperature of 70 °C were determined by comparing the peak values of XRD curves of

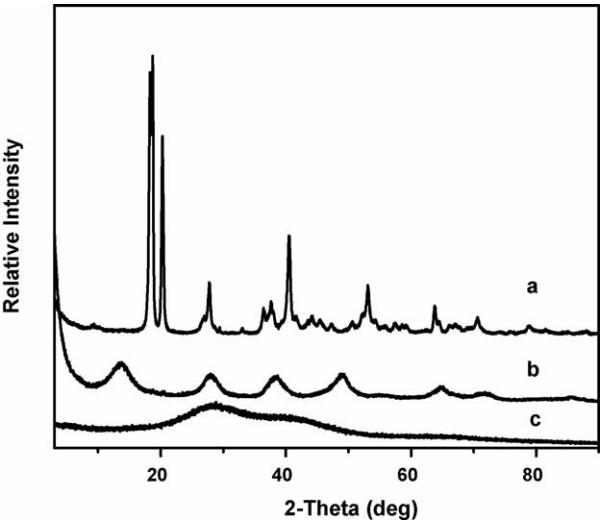

Fig. 10. XRD patterns of nano ATH (a), pseudoboehmite (b) and amorphous precipitate (c).

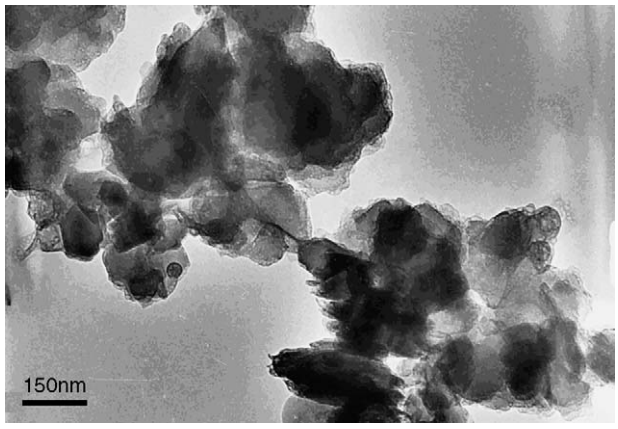

Fig. 11. TEM micrograph of thermal hydrolyzed ATH gels.

final products. TEM micrograph of ATH gel is illustrated in Fig. 11. By comparison between Figs. 2 and 11, it can be seen that the final product treated by high temperature drying are more condensed and regular morphology than ATH gel only treated by thermal hydrolysis.

3.7. Characteristics of product

The typical nano ATH product obtained under the above-mentioned optimum conditions was characterized by XRD, TEM and BET to show its crystal phase, particle morphology and surface area. XRD result shows that the product is gibbsite type of ATH, see Fig. 10. TEM photograph given in Fig. 12 indicates that the product has ultra thin hexagonal morphology with particle size of around 100–200 nm and thickness of 20–30 nm. The same product has a specific surface area of 29.7 m^2/g.

3.8. Carbonation process analysis

The carbonation process in RPB can be divided into three stages in terms of pH variation as shown in Fig. 13. In the induction stage, it is typical of a high [OH^-], in which case the acidification of CO_2 makes pH value gradually lowered,

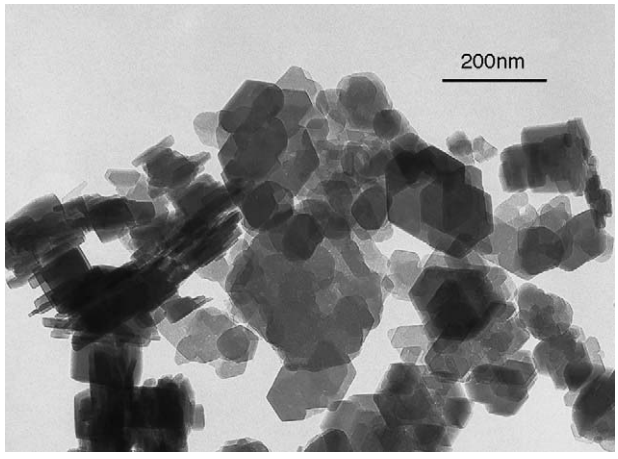

Fig. 12. TEM micrograph of well developed gibbsite particles of 150 nm (d_{50}) product.

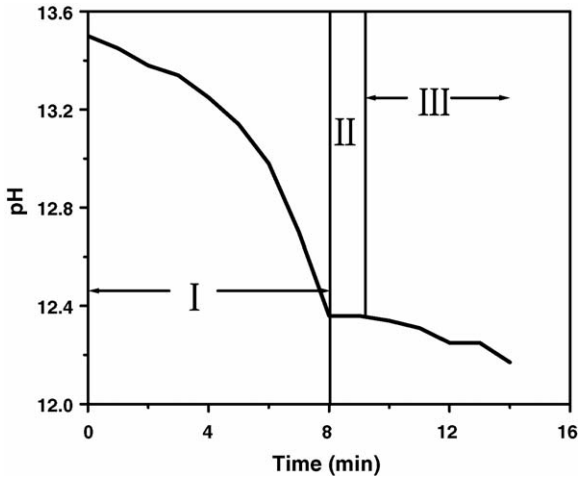

Fig. 13. pH variation in carbonation: (I) induction stage; (II) nucleation stage; (III) growth stage. Experimental conditions: $N = 360$ g; $[AlO_2^-] = 2.0$ mol/L; G/L = 1.0; $T = 25$ °C.

thereby accelerates the decomposition of $Al(OH_4^-)$ to accumulate $Al(OH)_3$ in the liquid phase, and finally the clear SA solution gradually becomes turbid. In the nucleation stage, as the supersaturation degree of $Al(OH)_3$ has exceeded the nucleating concentration, a great number of $Al(OH)_3$ nuclei are quickly generated out of the supersaturated SA solution. As a result, the reaction rate of step (2) instantaneously catches up with that of step (1), while the value of pH remains unchanged in the stage. In the growth stage, as the concentration of $Al(OH_4^-)$ has been very low, the reaction rate of step (2) is gradually lowered. ATH nuclei coalesce and grow to form the ATH colloids, as well as pH is gradually lowered by steps (1) and (2).

4. Conclusion

The process developed in the laboratory is essentially a controlled carbonation process of SA solution in a RPB reactor for synthesizing ultra thin hexagonal ATH particles. Based on the experiments done and discussions presented, the following major conclusions can be drawn.

1. RPB is beneficial to prepare nano-sized ATH gels with a narrow particle size distribution because the high gravity environment in RPB greatly intensifies both the CO_2 absorption and the micromixing process therein.
2. The product discharged from RPB was ATH colloids, which were subsequently treated by thermal hydrolysis and high temperature dryness to yield crystalline ATH product. The morphology of ATH particle is ultra thin hexagonal shape with diameter of 100–200 nm and thickness of 20–30 nm.
3. In carbonation process, operating conditions have significant effects on the preparation of nano ATH particles. It has been observed that low temperature favored finer product. In nucleation stage, the stabilization of pH is beneficial to create nano ATH gel, which is mainly determined by G/L and SA concentration. The higher the concentration of SA solution, the higher ATH productivity was obtained and the higher G/L should be corresponded with. In order to obtain nano ATH gel, final pH should be higher than 12.0.

Acknowledgment

The authors gratefully acknowledge the financial support provided by National “863” Program of China (No. 2002AA302605).

References

[1] T.J. Lynch, C. Tong, D. Riley, Advances in ATH benefit composite products, Reinforced Plastics 9 (2003) 44–46.
[2] L. Delfosse, C. Bailet, A. Brault, D. Brault, Combustion of ethylene–vinyl acetate copolymer filled with aluminium and magnesium hydroxides, Polym. Degrad. Stabil. 23 (1989) 337–347.
[3] G. Camino, A. Maffezzoli, et al., Effect of hydroxides and hydroxycarbonate structure on fire retardant effectiveness and mechanical properties in ethylene–vinyl acetate copolymer, Polym. Degrad. Stabil. 74 (2001) 457–464.
[4] F.Y. Wu, G.H. Liu, G.Z. Feng, Application and production of varieties aluminium hydroxide, Conserv. Utilization Min. Resour. Chin. 6 (2000) 41–44.
[5] U. Hippi, J. Mattila, M. Korhonen, J. Seppala, Compatibilization of polyethylene/aluminum hydroxide (PE/ATH) and polyethylene/magnesium hydroxide (PE/MH) composites with functionalized polyethylenes, Polymer 74 (2003) 1193–1201.
[6] C. Canaud, L.L.Y. Visconte, M.A. Sens, R.C.R. Nunes, Dielectric properties of flame resistant EPDM composite, Polym. Degrad. Stabil. 70 (2000) 259–263.
[7] X.G. Zhang, F. Guo, J.F. Chen, G.Q. Wang, H. Liu, Investigation of interfacial modification for flame retardant ethylene vinyl acetate copolymer/alumina trihydrate nanocomposites, Polym. Degrad. Stabil. 87 (2005) 411–418.
[8] J. Csige, J. Matyari, M.T. Banerjee, G. Kaptay, Light metals, in: The Minerals, Metals and Materials Society, TMS, Warrendale, PA, 1990.
[9] J.K. Pradhan, P.K. Gochhayat, I.N. Bhattacharya, S.C. Das, Study on the various factors affecting the quality of precipitated non-metallurgical alumina trihydrate particles, Hydrometallurgy 60 (2001) 143–153.
[10] K.A. Blanks, Novel synthesis of gibbsite by laser-stimulated nucleation in supersaturated sodium aluminate solutions, J. Cryst. Growth 220 (2000) 572–578.
[11] G. Lefevre, M. Fedoroff, Synthesis of bayerite (β-$Al(OH)_3$) microrods by neutralization of aluminate ions at constant pH, Mater. Lett. 56 (2002) 978–983.
[12] J.-F. Chen, et al., Interaction of macro and micro mixing on particle size distribution in reactive precipitation, Ind. Eng. Chem. Res. 39 (2000) 948–954.
[13] C. Ramshaw, Higee distillation—an example of process intensification, Chem. Eng. 13 (1983) 389–399.
[14] J.F. Chen, Y.H. Wang, K. Guo, F. Guo, C. Zheng, Synthesis of nano-cubic $CaCO_3$ by high-gravity reactive precipitation. 1. Experimental, Acta Metall. Sinica 35 (1999) 179–182.
[15] J.F. Chen, L. Shao, F. Guo, X.M. Wang, Synthesis of nano-fibers of aluminum hydroxide in novel rotating packed bed reactor, Chem. Eng. Sci. 58 (2003) 569–575.
[16] J. Li, Q.Y. Chen, Z.L. Yin, P.M. Zhang, Development and prospect in the fundamental research on the decomposition of supersaturated sodium aluminate solution, Prog. Chem. Chin. 15 (2003) 170–177.